International Journal of Advanced Geosciences, 12 (2) (2024) 84-97

International Journal of Advanced Geosciences

Website: www.sciencepubco.com/index.php/IJAG

Research paper

Seismic Inversion Techniques and Attribute Analysis for Accurate Well Placement in Offshore Niger Delta Basin, Nigeria

Tanguy W. Moukassa [1] *, Jerome E. Asedegbega [1, 2], Solomon A. Adekola [1, 3] Alexander Nwakanma [2]

[1] *Pan African University, University of Ibadan, Nigeria*
[2] *GCube Integrated Services Limited, Lagos, Nigeria*
[3] *Obafemi Awolowo University, Ile Ife, Nigeria*
**Corresponding author E-mail: tanguymoukassa@gmail.com*

Abstract

Before this study, simple methods like seismic attribute analysis have often been used for reservoir characterization with successes however, there is still the need to reduce exploration uncertainty to a negligible level and boost investors' confidence. This study integrated seismic inversion with seismic attribute analysis to better characterize the reservoirs in MTW Field in deep-offshore Niger Delta Basin. Five (5) wells with complete suite of petrophysical logs, three-Dimensional (3-D) seismic data, checkshot and other well information were used. The well data were thoroughly quality checked, reservoirs were litho-stratigraphically delineated and used for petrophysical analysis across the wells. This was followed by seismic-to- well-tie, seismic interpretation, and seismic attribute analysis (Root Mean Square-RMS) generated using depth surface maps. 3-D static reservoir model and volumetric evaluation were carried out. Petrophysical properties were derived and distributed across the 3-D static model using sequential gaussian simulation algorithm to ascertain shale volume spread across the model. To improve the seismic resolution and reduce interpretation uncertainty at greater depth, model- based post-stack seismic inversion was performed to obtain acoustic impedance cube. Litho-stratigraphic and petrophysical analysis result revealed five reservoir sands (A, B, C, D, and E). Reservoir-A was seen to be more viable with a thickness of 13.42 m, high effective porosity of 27%, permeability of 3187.53 mD, low water saturation of 34% and low shale volume of 11% which are indication good reservoir quality and producibility. The seismic interpretation revealed thirty-one (31) growth and antithetic faults oriented in the NE-SW and NW-SE directions, respectively. The RMS result revealed high amplitude reflectivity which is a measure of zone of interest. Based on this, seven (7) prospects and three (3) leads were identified. The seismic inversion result shows a high level of accuracy with a correlation coefficient of 0.997; 0.997; 0.995; and 0.996 in MTW-001, MTW-003ST1, MTW-004ST1 and MTW-005 wells, respectively. The acoustic impedance successfully resolved and improved on the resolution of the seismic stacking velocity especially at reservoir layers and at depth deeper than 3600 ms. Acoustic impedance as a layer property has improved on the lateral and vertical resolutions of the data beyond what the usual seismic interval velocity could image thus, validating some of the prospects and leads identified in this study. This demonstrated that uncertainty can be reduced by a blend of RMS and seismic inversion in identifying reservoir for accurate placement of wells. It is therefore recommended that E and P operators should adopt the technique in their future hydrocarbon exploration endeavor in frontier and matured basins.

Keywords: *3D Static Model; Model-Based Inversion; Acoustic Impedance Cube; Rock Properties.*

1. Introduction

One of the major challenges in hydrocarbon exploration is inaccurate well placement which has resulted in the drilling of dry holes and non-commercially viable prospects in all petroleum prolific basins in the world. This scenario has been encountered in data limited frontier areas and complex geologic settings like the inland, deep/ultra-deep offshore and deep onshore prospects in Nigeria basins. Prior now, simple methods like seismic attribute analysis have often been used for reservoir characterisation with successes. However, it usually raises the cost of hydrocarbon exploration and increase the risk associated with development and production in offshore areas (Olowoyo, 2010). Several publications have shown that these risks can be reduced using seismic inversion techniques to improve the seismic resolution of conventional seismic data combined with attribute analysis. Transforming seismic interval to rock layer properties has proven to be useful to evaluate the property conditions of reservoir and de-risk the entire prospect.

This study is, therefore, based on integrating attribute analysis with seismic inversion workflow for enhanced reservoir characterization and accurate well placement.

2. Geology of Niger Delta Basin

The Niger Delta is located in the Gulf of Guinea and part of West Africa Rifting System as described by Klett et al., (1997). The south-westward progradation of Delta from the Eocene to present, generated depobelts which reflect the most active region of Delta at each stage of its history (Doust and Omatsola, 1990) (Fig. 1). The Delta extends around 300,000 km^2 (Kulke, 1995) and has 500,000 km^3 of sediment volume (Hospers, 1965) with 10 km of sediment thickness in its depocenter (Kaplan et al.,1994). These Depobelts represent one of the biggest regressive deltas in the world. The petroleum system identified until today in the Niger Delta province is called the Tertiary Niger Delta (Akata-Agbada) (Kulke, 1995; Ekweozor and Daukoru, 1994). It is also the tenth richest in petroleum resources among the provinces rated in the US Geological Survey's World Energy Assessment (Klett et al., 1997), with 2.2 % of oil and 1.4 % of gas discovered in the world (Petroconsultants, 1996). The minimum extent of this system is determined by field comprising known reserves (cumulative production plus proved reserves) of 34.5 billion barrels of oil (BBO) and 93.8 trillion cubic feet of gas (TCFG), 14.9 billion barrels of oil equivalent (BBOE) (Petroconsultants, 1996). The petroleum component is as result of organic matter transformation from the original state to kerogen, then to hydrocarbon under the high temperature, pressure, and chemical conditions deposited throughout sediments in a favorable environment. (Evamy et al., 1978) set the top of the present-day oil window in the Niger Delta at the 240° F (115° C) isotherm. In the northwestern portion of the delta, the oil window (active source rock interval) lies in the upper Akata Formation and the lower Agbada Formation. To the southeast, the top of the oil window is stratigraphically lower, up to 4000 m below the upper Akata/lower Agbada sequence (Evamy et al., 1978; Nwachukwu and Chukwurah, 1986; Doust and Omatsola, 1990). Stacher, 1995 attributed the distribution of the top of the oil window to the thickness and sand/shale ratios of the overburden rock (Benin Formation and variable proportions of the Agbada Formation). The sandy continental sediment (Benin Formation) has the lowest thermal gradient (1.3 to 1.8°C/100 m), the paralic Agbada Formation has an intermediate gradient (2.7°C/100 m); and the marine, overpressured Akata Formation has the highest (5.5°C/100 m) (Ejedawe et al., 1984). Therefore, within any Depobelts, the depth to any temperature is dependent on the gross distribution of sand and shale. If the sand/shale ratio was the only variable, the distal offshore subsurface temperature would be elevated because of the lower percentage of sand. According to Beka et al., 1995, the depth of the hydrocarbon kitchen is expected to be greater than the depth of the delta itself, because the depth generation of the oil depends on associated factors like time, tectonic deformation, and temperature.

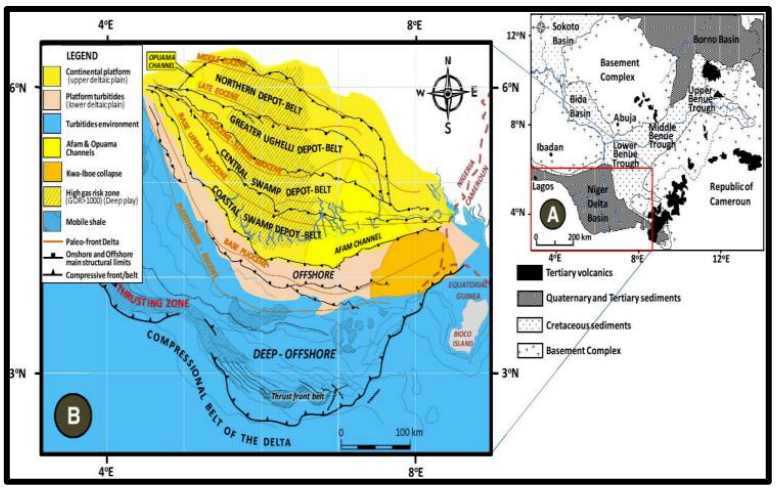

Fig. 1: Geologic Map of Nigeria Showing the Location of the Niger Delta Basin and Sectional Map of the Niger Delta Depobelts and Structural Limits (Doust and Omatsola, 1990).

3. Location of study area

The study area is found within the offshore Niger Delta basin in Nigeria (Fig. 2). The field lies between longitude 4°35'53.137"E and latitude 4°33'2.368"N, located within the deep offshore depobelt of the Niger Delta.

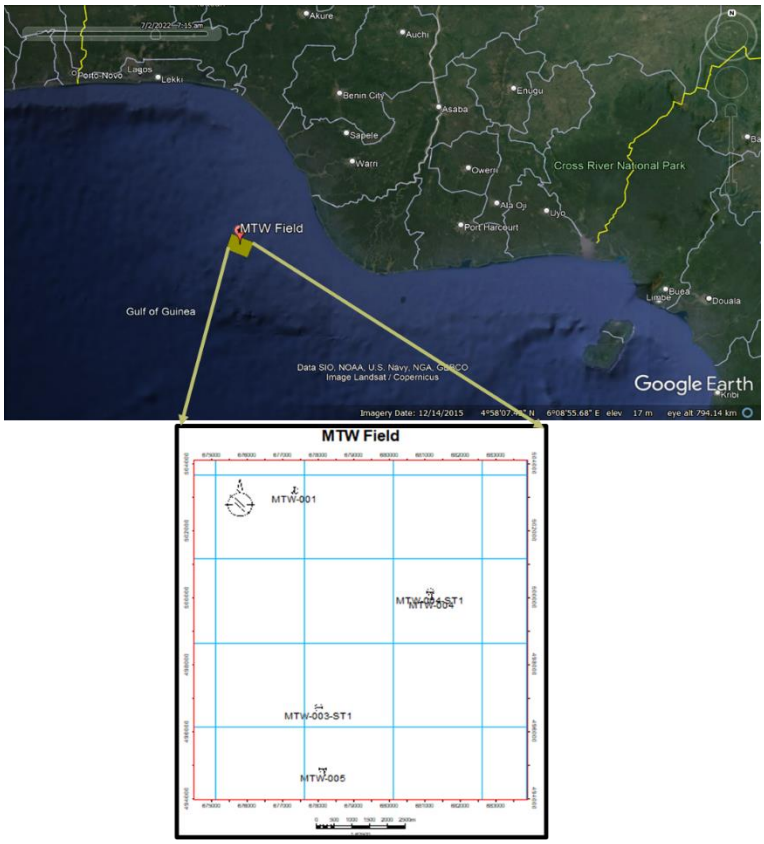

Fig. 2: Map of the Location of MTW-Field, in Offshore Niger Delta Basin (Adapted from Google Earth 2021) and the Base Map for MTW-Field Showing the Distribution of Wells Across the Field of Study

4. Theoretical framework

4.1. Well logs

The well log refers to borehole logging and serves to record different events crossed during a drilling process. It will mention the formation penetrated using the crossplot formation versus the depth, to know with exactitude where the formation is coming from a particular depth during a drilling. Specifically, the logging records the magnitude of different formation crossed, using natural emission of radioactive, resistivity, it has also a chart showing different values that can be measured and plotted with depth.

4.2. Types of well logs

4.2.1. Gamma ray log

Gamma ray log measures the natural radioactive emissions of rock and helps to identify the lithology and to correlate different zones that have the same rock types. For instance, the shale formation has the high concentration radioactive elements, so the gamma ray readings will have high API value, contrary to sandstone and carbonate which have lower concentration radioactive elements, the readings will be lower compared to shale formation.

4.2.2. Resistivity log

The resistivity measures the resistance of a formation, material to the flow current, basically it is inverse of conductivity. The resistivity depends on electrical conductivity of the rock, how the material resists the flow current within the formation, water (fresh or brine), oil, and gas.

4.2.3. Density log

Density log is a porosity log which help to indicate the presence of fluids within the pores space, it is also a lithology indicator. Density log used two different values of density: The bulk density (ρb or RHOB) which is the value of entire formation (solid and fluid parts) and the matrix density (ρma) is for the solid rock formation such as sandstone or limestone. Density can be estimated using the equation.

$$\emptyset_{\text{Den}} = \frac{\rho_{\text{ma}} - \rho_{\text{b}}}{\rho_{\text{ma}} - \rho_{\text{f}}} \quad (1)$$

ϕ_{Den} = Apparent density porosity
ρ_{ma} = Matrix density
ρ_b = Bulk density log reading
ρ_f = Fluid density (1.1 salt mud, 1.0 fresh mud and 0.7 gas)

4.2.4. Neutron log

A neutron log is also a porosity log that measures hydrogen concentration within the formation and liquid filled porosity (φN, or NPHI). It also defines the presence of fluids content, such as oil, gas, water within the pores space. The relationship between the neutron count rate and porosity can be expressed mathematically as

$$log_{10} \emptyset = aN + B \quad (2)$$

a = constant
B = constant
N = count rate and ϕ is the true porosity.

3.2.5. Sonic log

Sonic log is a porosity log that measures the interval transit time (Δt or DT) of a compressional sound wave moving through the formation throughout of the borehole. The interval transit time (Δt) is measured in microseconds per foot or microseconds per meter (μsec/ft, μsec/m), which is reciprocal value of the velocity of a compressional sound wave in feet per second. Sonic logs can be mathematically as;

$$\emptyset_{Sonic} = \frac{\Delta t\, log - \Delta tma}{\Delta t_f - \Delta tma} \times \frac{1}{C_p} \quad (3)$$

ϕ_{Sonic} = Sonic derived porosity
Δt_{ma} = interval transit time of matrix (given)
Δt_{log} = Interval transit time of formation
Δt_F = Interval transit time of fluid in the well bore (Fresh mud = 189, salty mud = 185)

$$C_p = \frac{\Delta t_{sh} \times c}{100} \quad (4)$$

C_p = compaction factor
Δt_{sh} = Interval transit time of adjacent shale
C = a constant, normally 1.0 (Hilchie, 1978)

4.3. Petrophysical properties estimation

The study of the physical and chemical characteristics of rock, as well as their interactions with fluids, is known as petrophysics. It is primarily used in the petroleum sector to analyze reservoir features such as Gross and Net thickness, fluid saturation, permeability, porosity, Net-to-Gross ratio, and shale volume. Measuring and interpreting these rock parameters via well log measurements is an important element of petrophysics. The following are the petrophysical properties:

4.3.1. Gross and net thickness

The gross thickness of the reservoir is the whole interval of the reservoir, including the shaly parts, whereas the net sand is the thickness of clean sand in the reservoir with no shaly components. After determining the volume of shale and subtracting it from the overall reservoir interval, the net sand may be calculated.

4.3.2. Porosity

Depending on whether it includes porosity associated with clays, porosity can be characterized as effective or total; certain techniques estimate total porosity and must be adjusted for clay content. The following equation was used to compute total porosity (T) and effective porosity (E):

$$\emptyset_T = \frac{\rho_{ma} - \rho_{bulk}}{\rho_{ma} - \rho_{fl}} \quad (5)$$

$$\emptyset_E = \emptyset_T - (\emptyset t_{sh} \times Vsh) \quad (6)$$

Φ_T = density derived porosity
ρ_{ma} = matrix density taken as 2.65g/cm^3
ρ_{bulk} = matrix density taken as bulk density log values
ρ_{fl} = fluid density taken as 1.00g/cm^3
V_{sh} = Shale volume
Φ_{tsh} = Total porosity of shale

4.3.3. Fluid saturation

In petrophysics, fluid saturation includes both water and hydrocarbon saturation levels. Water saturation (Sw) is the fraction of total pore volume saturated by formation water; for water saturation (Sw), the empirical equation from Archie's (1942) was used as follows;

$$Sw = \left(\frac{a \times R_w}{R_t \times \emptyset_t^m}\right)^{1/n} \quad (7)$$

S_{wa} = Archie's water saturation for clean sand

a = Tortuosity factor that is 1
m = Cementation exponent which is 2
n = Saturation exponent that is 2
Rt = Formation resistivity (read from log)
Rw = Formation water resistivity (read from log)
Φ_t = Total Porosity
The fraction of fluid (oil and gas) that is saturated with hydrocarbons is obtained using

$$S_H = 1 - S_w. \quad (8)$$

4.3.4. Permeability

Permeability (K or k) is a measure of a reservoir's potential to conduct fluids or allow flow between the reservoir and a wellbore. It is dependent on the associated rock and fluid properties and is one of the most complicated to evaluate and quantify without data at all pertinent scales - core, log, and production test. This is measured in darcies (D) but is commonly reported in millidarcies (mD). Permeability (K) is calculated using the equation as follows;

$$K(mD) = 307 + 26552\,(\emptyset^2) - (\emptyset \times S_w)^2 \quad (9)$$

4.3.5. Net-to-gross

This is the total pay interval divided by the reservoir's entire interval. One method of estimating N/G is to compute the oil initially in place (OIIP) or gas initially in place (GIIP) assuming that the whole reservoir thickness is utilized to estimate the total volume of hydrocarbons contained. Net-to-Gross is an indicator of the productive capacity of a reservoir and can be estimated as.

$$\text{Net-to-gross} = \frac{NT}{GT} \times 100 \quad (10)$$

NT = Net thickness
GT = Gross Thickness
The higher the Net to Gross, the better the reservoir quality.

4.3.6. Shale volume

The amount of shale in a reservoir has an important influence in hydrocarbon production; the higher the reservoir shaliness, the lower the reservoir productivity. The following equation for tertiary sands is used to compute shale volume:

$$Vsh = 0.083 * (2^{(3.7 * GR_{index})} - 1) \quad (11)$$

GR log = GR log reading
GR min = GR sand baseline
GR max = GR shale baseline

4.4. Surface attribute

Surface attribute is considered by geoscientists, a key tool for reservoir quality control and characterization, because it reveals the seismic features and anomalies, patterns, and relationships. It divided into two objectives ‘’geometrical attribute for visibility enhancement of seismic characteristics and physical attribute related to lithology’’ (Othman et al., 2017). There are several surface attributes (RMS, maximum amplitude, average energy) but for this study we focused on RMS amplitude extraction.

4.5. Seismic inversion

Geophysicists utilize seismic inversion to construct subsurface rock characteristics models utilizing seismic and well log data. It should be emphasized that seismic inversion enhances the resolution of original or conventional seismic data. It is separated into two techniques: pre-stacking (simultaneous and elastic inversion methods) and post-stacking inversion (Veeken et al., 2004) (coloured inversion, model-based inversion, sparse spike inversion and Band-limited impedance inversion methods).

4.5.1. Post-stack inversion

To construct the inverted acoustic impedance for rock attributes, this approach employed a single seismic trace (initial model) wavelet related with reflectivity plus noise. It was used to improve seismic data resolution and interpretability by eliminating incoherent noise (Farfour et al., 2015). This method is extensively used in the oil and gas sector to get layer attributes for stratigraphic interpretation (Maurya et al., 2016; Veeken and Da Silva, 2004). The acoustic impedance is the multiplication of bulk density and sonic velocity, which help to predict the rock properties of subsurface such as the lithology, porosity, and fluid content.

5. Methodology

5.1 Materials and methods

This study employed 3-D seismic and well logs data acquire from the MTW Field in the Offshore, Niger Delta area. The suites of log used were principally gamma ray log, neutron, density, sonic, and resistivity logs from five (5) wells. The seismic data used in this study was a

3-D post-stack seismic data with a wavelet type of zero phase and SEG reverse polarity. The inline ranges from 2099 to 3799, corresponding to crossline ranges from 2110 to 4510 with a line spacing of 25 meters.

5.2. Research workflow

The workflow is detailed as seen in Figure 3 below.

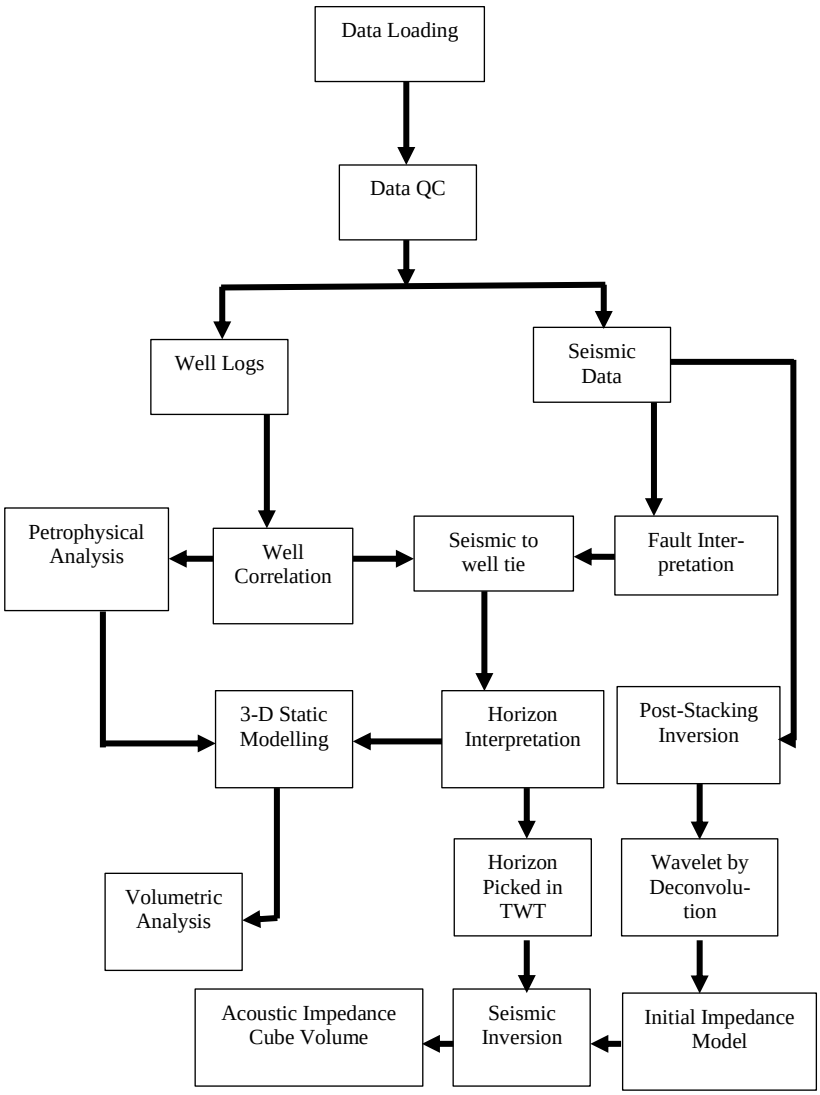

Fig. 3: Integrated Workflow Utilized for the Analysis of MTW-Field

5.3. Methods

The data set was quality checked and sorted into an acceptable format and were used for well correlation, petrophysical analysis, seismic interpretation, surface attribute extraction, 3-D static model and seismic inversion. The data loading method's chronology was as follows: Well header, well deviations survey in well path/deviation ASCII (*.*) file type, well logs in Las format, checkshot in ASCII (*.*), seismic section in SEGY format, thus each file was reviewed for inaccurate values and discarded for quality control.

5.3.1 Well Logs Correlation

The correlation of wells was performed using gamma ray log readings to differentiate the reservoir and non-reservoir. The petrophysical analysis based on shale volume, effective porosity, permeability, net-to-gross, water and hydrocarbon saturations were accurately derived for each of the wells used in MTW Field to estimate their average values, the amount of hydrocarbon and predict the quality of each reservoir, as shown in Figure 4.

5.3.2 Seismic Interpretation

The structural interpretation which is covered by fault mapping performed on seismic smoothing as volume attributes in inline, after mapping on variance attribute used to improve the seismic amplitudes and discontinuities along the entire seismic section. The seismic mapping was done along the entire seismic section. The identification of faults was carried out following the discontinuities of layers where minor and major discontinuities were discovered and selected on seismic lines.
To generate synthetic seismogram, seismic to-well-tie was done for mapping the horizons at top and base of each reservoir across the inline and crossline of seismic. Structural smoothing attribute was generated to increase the visibility of event on the seismic. Horizons mapped were converted to time surfaces, then velocity model was utilized to covert the time surfaces to depth surfaces.

5.3.3. Surface attribute

Root-mean square (RMS) as a surface attribute was extracted from two-time surfaces mapped, to aid the identification of hydrocarbon prospects on the surfaces generated.

5.3.4. 3D Static modelling

After depth surfaces were generated, 3-D static modelling was built by carrying out the following processes namely, fault modelling, horizon modelling, pillar gridding, property modelling (well log upscaling), petrophysical modelling, fluid contacts, and volume of fluids.

5.3.5. Seismic inversion

The inversion workflow was carried out using the following procedure: selection of the post-stack seismic and interpreted horizons, extraction of statistical wavelet, selection of the well to be used, correlation of the wells, building the initial model, inversion analysis, and generation of the 3-D acoustic impedance cube.

6. Results and discussion

Results obtained from this study include well correlation, petrophysical properties estimation, surface attribute analysis, 3-D static modelling, and seismic inversion.

6.1. Well correlation

Five lithological reservoirs were identified from the correlation results as seen in Figure 4 below, with the emphasis on the reservoir of interest for this study being reservoir MTW A. Reservoir MTW A in the four wells revealed based on gross thickness and significant pay zone interval ranging from 2819.89 m to 2834.53 m for well MTW-001, 1977.74 m to 1997.63 m for well MTW-003 ST1, 2500.92 m to 2506.69 m for MTW-004 ST1, and 2402.53 m to 2411.92 m for well MTW-005 for the reservoir top and base respectively.

6.2. Petrophysical properties estimation

The litho-stratigraphic correlation panel as showed in Figure 4 below with five (5) reservoir units (MTW A, MTW B, MTW C, MTW D, and MTW E) identified. Table 1 shows the results of the petrophysical properties estimation and evaluation for all five wells across the five reservoir units identified in the field while Table 2 shows the estimated average value of the petrophysical properties for five reservoirs across all wells. From this analysis, reservoir A was revealed to be more viable amongst all other reservoirs evaluated, with thickness of 13.42 m high effective porosity of 27%, permeability of 3187.53 mD, low water saturation of 34% and low shale volume of 11% which indicates a good reservoir quality and producibility for hydrocarbon accumulation.

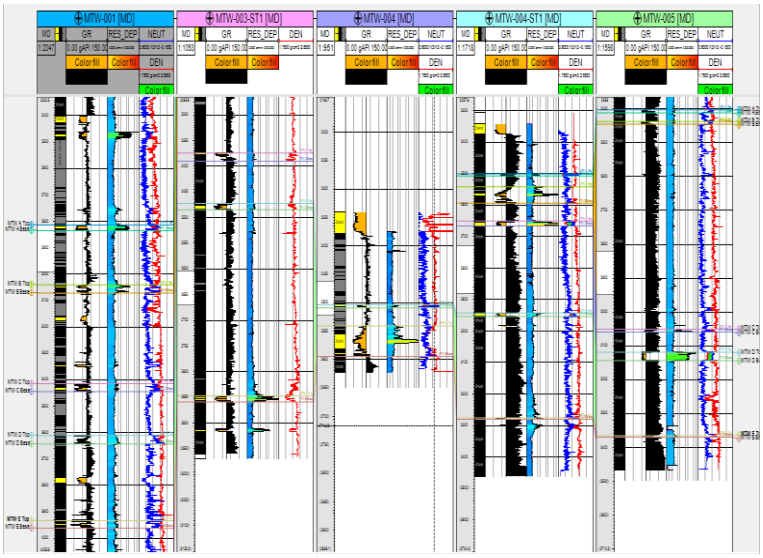

Fig. 4: Lithostratigraphic Correlation of the Five Reservoirs Across the Five Wells in the Field

Table 1: Results of Petrophysical Evaluation of Five Reservoir Units for Five Wells in the MTW Field

Well	Reservoirs	Top (m)	Base (m)	Gross Thickness (m)	Vsh (%)	Vsh (m)	Net Sand (m)	Net-to-Gross (%)	PHIT (%)	PHIE (%)	Sw (%)	Perm (mD)	Hydrocarbon Saturation (%)	Fluid type
MTW-001	A	2815.89	2834.53	18.64	9.14	1.70	16.94	90.86	20.95	18.68	37.49	3,441.24	62.51	Oil/water
	B	3041.33	3071.84	30.51	9.13	2.79	27.72	90.87	17.91	16.18	52.25	1,990.73	47.75	Oil/water
	C	3414.24	3446.44	32.20	9.45	3.04	29.16	90.55	18.18	16.45	66.02	1,439.29	33.98	Oil/water
	D	3622.03	3643.52	21.49	10.12	2.18	19.32	89.88	19.70	18.05	46.27	1,066.61	53.73	Oil/water

	E	3933.15	3964.09	30.94	9.22	2.85	28.09	90.79	18.67	17.63	48.45	1,285.86	51.55	Oil/water
MTW-003 ST1	A	1977.74	1997.63	19.89	8.13	1.62	18.27	91.87	45.69	41.09	28.45	5,505.74	71.55	Oil/water
	B	2083.37	2123.59	40.22	9.70	3.90	36.32	90.30	36.24	33.42	31.32	2,099.95	68.68	Oil/water
	C	2373.74	2390.09	16.35	12.92	2.11	14.24	87.09	29.88	26.95	37.54	2,393.40	62.46	Oil/water
	D	2472.30	2484.23	11.93	11.20	1.34	10.59	88.80	26.72	24.44	34.86	2,263.04	65.14	Oil/water
	E	2846.65	2859.02	12.37	9.13	1.13	11.24	90.88	34.81	31.71	27.95	2,854.31	72.05	Oil/water
MTW-004 ST1	D	2503.88	2509.07	05.19	9.80	0.51	4.68	90.20	35.09	32.18	20.89	3,400.73	79.12	Oil/water
	E	2540.20	2594.09	53.89	9.52	5.13	48.76	90.48	31.46	28.89	34.48	2,676.35	65.52	Oil/water
MTW-004 ST1	A	2500.92	2506.69	05.77	15.31	0.88	4.89	84.69	28.80	23.41	39.42	2,001.83	60.58	Oil/water
	B	2554.29	2593.96	39.67	9.38	3.72	35.95	90.63	28.80	26.50	30.75	1,621.91	69.25	Oil/water
	C	2650.23	2666.09	15.86	9.73	1.54	14.32	90.27	30.28	26.87	35.93	3,458.17	64.08	Oil/water
	D	2943.07	2953.89	10.82	12.12	1.31	9.51	87.88	23.11	20.47	39.15	2,249.04	60.85	Oil/water
	E	3275.59	3279.92	04.33	08.58	0.37	3.96	91.42	18.36	15.52	45.54	2,069.64	54.47	Oil/water
MTW-005	A	2402.53	2411.92	09.39	09.66	0.91	8.48	90.34	30.79	26.20	31.82	1,801.33	68.18	Oil/water
	B	2435.40	2444.12	08.72	10.64	0.93	7.79	89.37	31.61	29.94	27.63	2,570.49	72.37	Oil/water
	C	3053.90	3058.59	04.69	17.24	0.81	3.88	82.76	34.30	29.36	36.96	2,675.48	63.04	Oil/water
	D	3119.64	3144.46	24.82	17.33	4.30	20.52	82.68	28.90	25.57	35.78	2,588.14	64.22	Oil/water
	E	3365.83	3369.86	04.03	16.51	0.67	3.37	83.50	24.57	21.84	45.72	2,029.76	54.29	Oil/water

Table 2: Estimated Average Value of the Petrophysical Properties for Five Reservoirs Across all Wells

Reser-voirs	Gross Thickness (m)	Vsh (%)	Vsh (m)	Net Sand (m)	Net to Gross (%)	PHIT (%)	PHIE (%)	Sw (%)	Perm (mD)	Hs (%)
A	13.42	10.56	1.28	12.15	89.44	31.56	27.34	34.30	3187.53	65.71
B	29.78	9.71	2.83	26.95	90.29	28.64	26.51	35.48	2070.77	64.51
C	17.28	12.33	1.88	15.40	87.67	28.16	24.90	44.11	2491.58	55.89
D	14.85	12.11	1.93	12.92	87.89	26.70	24.14	35.39	2313.51	64.61
E	21.11	10.59	2.03	19.10	89.41	25.57	23.12	40.43	2183.18	59.57

6.3. Surface attributes analysis

The structure contour map also revealed the presence of anticlinal structure on the two surfaces generated, which could be considered the main hydrocarbon trapping mechanism within the field (Fig. 5). The high reflectivity of amplitude observed on RMS amplitude surface A as shown in Figure 6 precisely, in the northeastern part of map (Fig. 6) with travel time ranging from 2500 to 4700 ms at contour interval of 100 ms, is an indication of hydrocarbon prospect. Seismic anomaly (dim spot) was observed in the southern and southeastern parts of the map of surface B (Fig. 6). At the intervals of dim spot between 2500 to 4800 ms at contour interval of 100 ms low acoustic impedance was pronounced due to the presence of hydrocarbon as can be seen in Figure 6.

6.4. 3D Static modelling

The results from the 3-D model were spatially distributed across the reservoir using petrophysical properties such as Net-To-Gross (NTG), shale volume, effective porosity, permeability, and water saturation are as follows.

6.4.1. Net-to-gross model

The reservoir model was filled with an average petrophysical value for NTG ranging from 50 to 97% to depict the dispersion of these values over the reservoir region. The distribution of NTG values ranging from low (0.1 - 0.2) was seen in blue and purple color for places with low net-to-gross. This increase to average (0.2 - 0.6) is displayed in light blue and green colors, whereas (0.6 - 0.9) is shown in yellow and red colors in figure 7. The reservoir's NTG is believed to be high due to a dense population of average to high value over the reservoir.

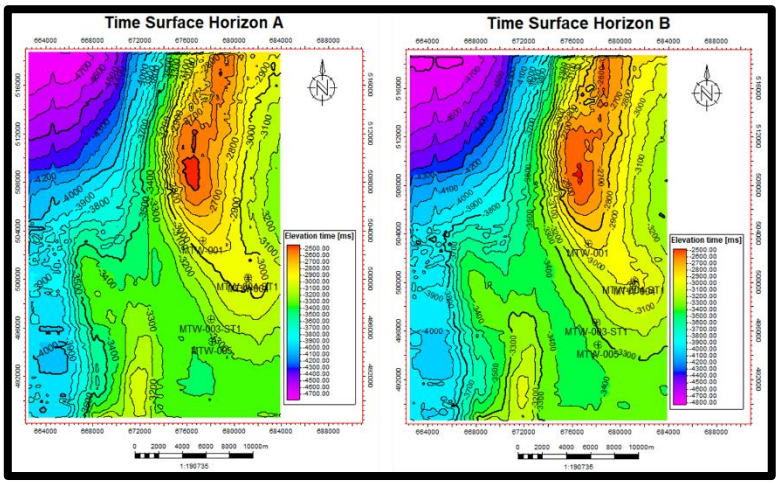

Fig. 5: Time Structural Map for Horizons A And B

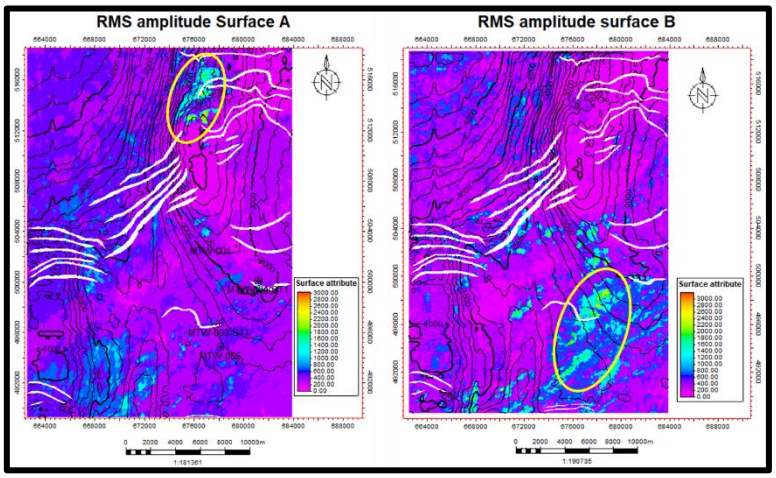

Fig. 6: RMS Seismic Attribute Extracted for Horizons A and B

6.4.2. Shale volume model

With an average petrophysical value ranging from 20-35%, shale volume as shown in figure 8 depicts the distribution of sand and shale area, with sand regions ranging below 7.5% (light brownish color), shaly sand areas ranging between 7.5 – 22.5 % (brownish colour) and shale rich areas reaching above 22.5 % (dark brownish colour).

6.4.3. Effective porosity model

Haven distributed an average petrophysical value ranging from 0.10 – 0.45 fraction for the effective porosity model, the pale yellow to orange colors suggest a particularly acceptable range of 0.25 - 0.30 for efficient porosity. Effective porosity values greater than 0.30 fraction, as seen in blue to pink colouration (fig. 9), indicate that the reservoir is exceptionally porous and serves as an excellent feature for retaining hydrocarbon.

6.4.4. Permeability model

Figure 10 depicts the reservoir's predicted permeability, which ranged between 1066 to 5600 mD based on petrophysical study. The observed model showed low permeability (< 250 mD) as shown in purple colour, extraordinarily good (>250 - 1000) mD in light blue while areas with excellent (> 1000 mD) permeability values seen in green to yellow colors were evenly distributed across the reservoir. These findings indicate that this reservoir meets the requirements for economic hydrocarbon production.

6.4.5. Water saturation model

Water saturation which reveals the fraction of total pore volume occupied by formation water was dispersed over the average petrophysical property range of 30 - 60% (fig. 11). The model was observed to be densely populated with low water saturation values between 5 – 35 % (orange to light green colours).

6.4.6. Reservoir oil-water contact (OWC)

Hydrocarbon accumulates in a reservoir over time owing to migration, timing, and a strong sealing mechanism. Within the pore spaces of the reservoirs, three fluids exist: gas, oil, and water (fresh or brine), or a mix of the two. The reservoir's OWC was visualized at -1947.24 ft to distinguish the zone of production from the zone of high-water saturation. Figure 12 depicts the model with areas highlighted in green as areas of hydrocarbon production in the reservoir and areas marked in blue as non-productive sections of the reservoir. The results show all existing wells so afar penetrated hydrocarbon yielding zones and may be producible.

6.4.7. STOIIP estimation

For STOIIP evaluation, nine instances were simulated to evaluate and assess the average of stock tank oil originally in place (STOIIP), which demonstrates a good quantity of hydrocarbon reserve for Reservoir Nel_1902. The results revealed that the reservoir's hydrocarbon production capacity averagely ranged from 13.2 – 14.5 MMstb and reserve of 22.02 - 23.54 MMbo (Table 3).

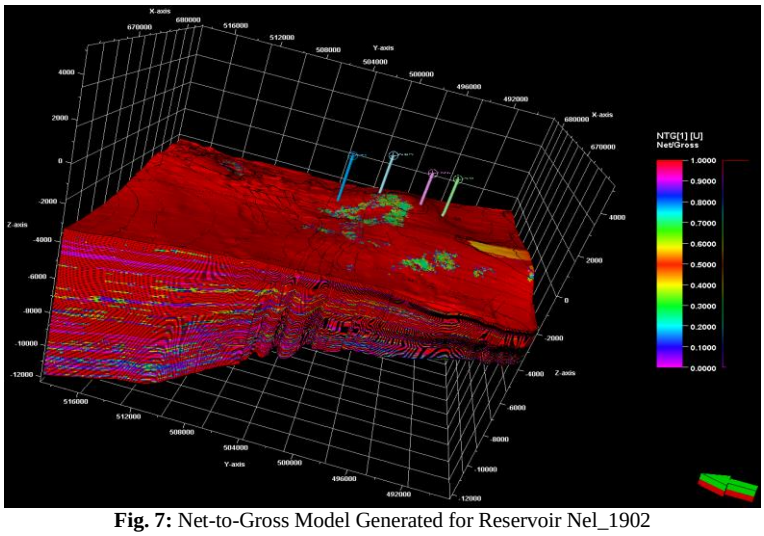

Fig. 7: Net-to-Gross Model Generated for Reservoir Nel_1902

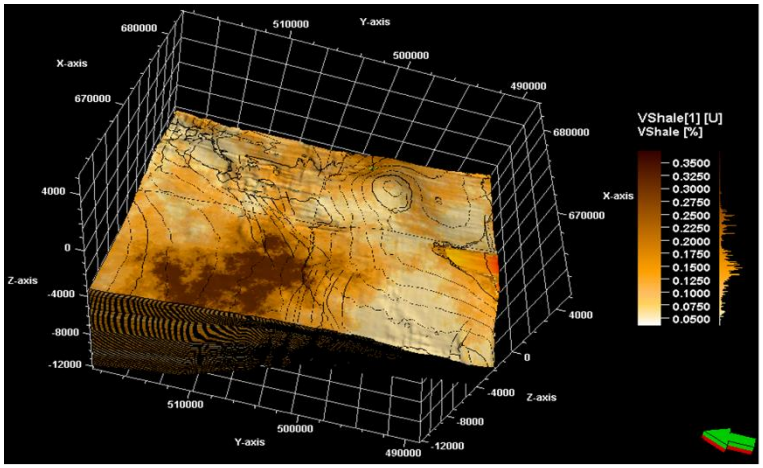

Fig. 8: Shale Volume Model Generated for Reservoir Nel_1902

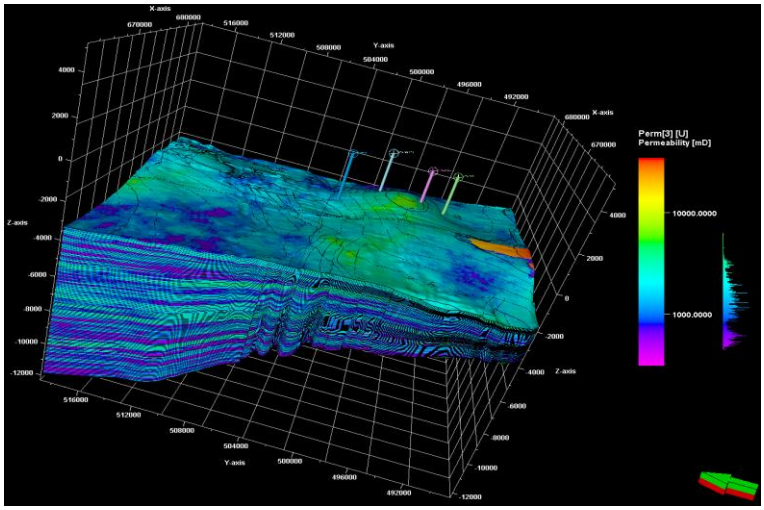

Fig. 9: Permeability Model Generated for Reservoir Nel_1902

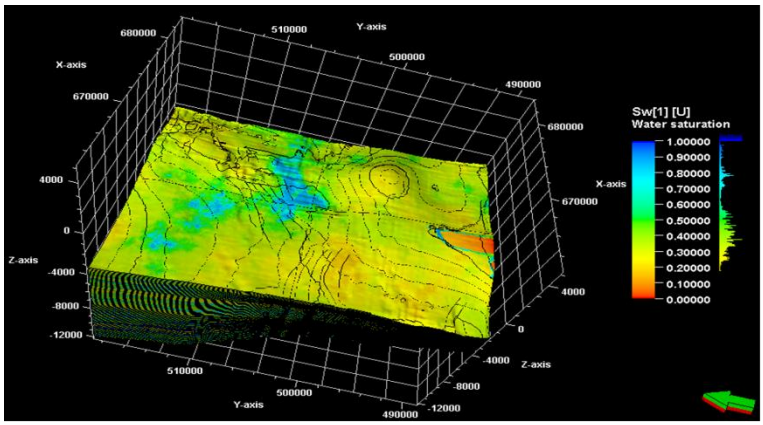

Fig. 10: Water Saturation Model Generated for Reservoir Nel_1902

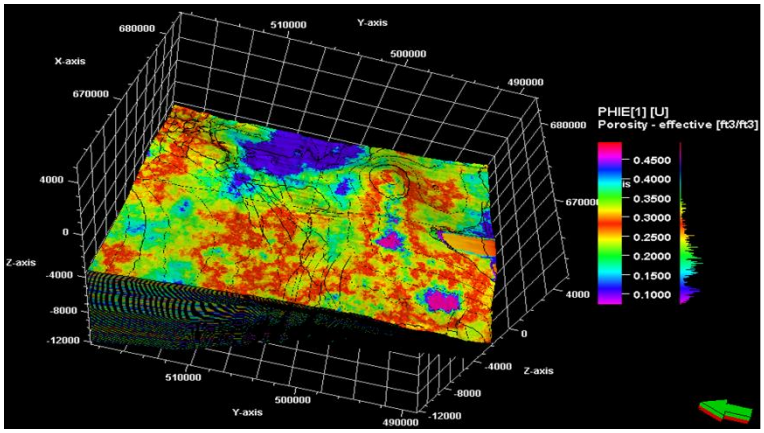

Fig. 11: Effective Porosity Model Generated for Reservoir Nel_1902

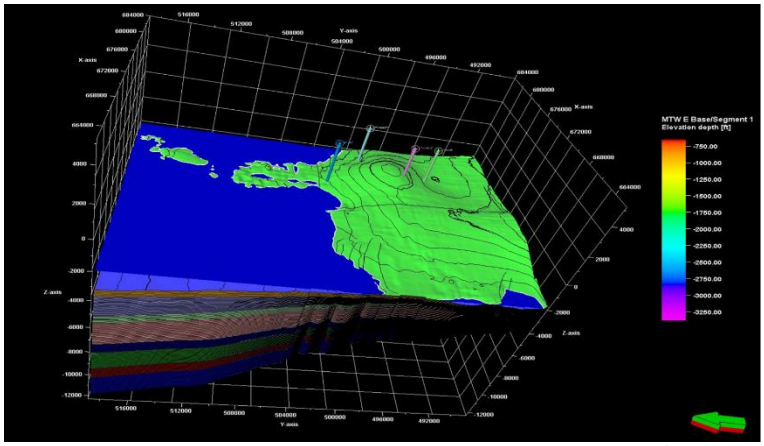

Fig. 12: Oil-Water Contact (OWC) Model, Delineating Oil and Water (Brine) for Reservoir

Table 3: STOIIP Values Simulated for Nine Cases in Reservoir Nel_1902

Items	STOIIP_in_oil _10^6_STB_	Recoverable_oil _10^6_STB_	Pore_volume _10^6_STB_	Net_volume _10^6_ft3_	HCPV_oil _10^6_RB_	Bulk_volume _10^6_ft3_
Case1	135996.56	135996.56	452718.25	13805467.54	224394.32	17854904.85
Case2	133597.21	133597.21	450192.74	13451475.38	220435.40	17854904.85
Case3	142355.59	142355.59	468983.68	13669692.63	234886.73	17854904.85
Case4	140841.55	140841.55	471615.22	13756367.10	232388.55	17854904.85
Case5	133891.75	133891.75	446041.03	13388080.73	220921.38	17854904.85
Case6	142259.05	142259.05	471475.44	13851745.29	234727.43	17854904.85
Case7	133512.61	133512.61	442512.84	13438953.15	220295.81	17854904.85
Case8	139978.28	139978.28	457537.94	13717681.26	230964.15	17854904.85
Case9	142681.01	142681.01	464067.69	13714822.82	235423.66	17854904.85

6.5. Seismic inversion

Wavelet extract revealed maximum correlation of 0.415, 0.497, 0.322, and 0.159 for MTW-001, MTW-003ST1, MTW-004ST1 and MTW-005 wells respectively. The inversion analysis revealed a high correlation of 0.996744 between the original seismic data and synthetic seismic trace. Seismic prediction error estimated was very low, about 0.0810005 boosting the simulation confidence level. Acoustic impedance was observed to increase with depth, with anomalous areas revealing a reverse in acoustic impedance value (Fig. 13). 3-D acoustic impedance cube effectively resolved reservoir layers with low acoustic impedance values where, high porosity pointed sand zones with

non-reservoir layers depicting high acoustic impedance values (i.e., low porosity pointing shale-rich zones or shaly sand) as shown in Figure 14. Higher impedance value right below MTW B base interpreted horizon with impedance value between 5883 - 7554 ((m/s)*(g/cc)) depict probable shale rich areas across the field (light blue to purple colour), spread across from West to East of the field while lower impedance which depict probable sand rich areas (green to red colour) fall between 3545 - 5800 ((m/s)*(g/cc)) (Fig. 14). Inverted acoustic Impedance log distributed across the 3-D model showed that much more saturation of prospective hydrocarbon accumulation exists around areas depicted from yellow to red colour. Low P-impedance revealed high porosity areas on the model -3250 to -2250 [g.ft/(cm3.s)], while shale rich beds were characterized by high P-impedance values from -2000 to -750 [g.ft/(cm3.s)] seem between green and blue colours (Fig. 15).

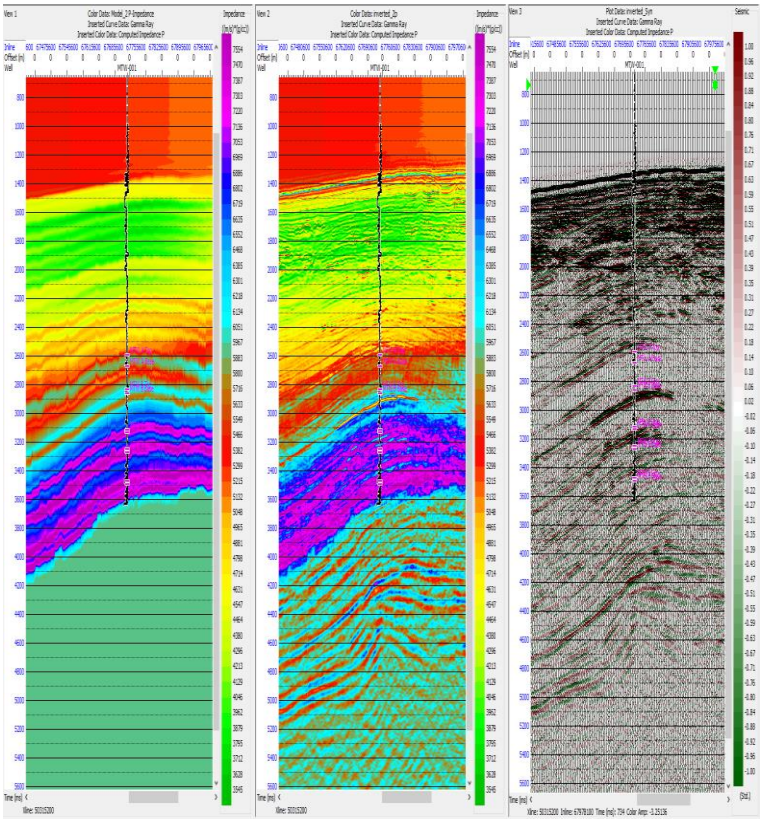

Fig. 13: Post-Stack Inversion Result Showing the Initial Model (Left), the Inverted Acoustic Impedance (Center) and the Seismic Stacking Velocity (Right) with MTW-001 Well Inserted.

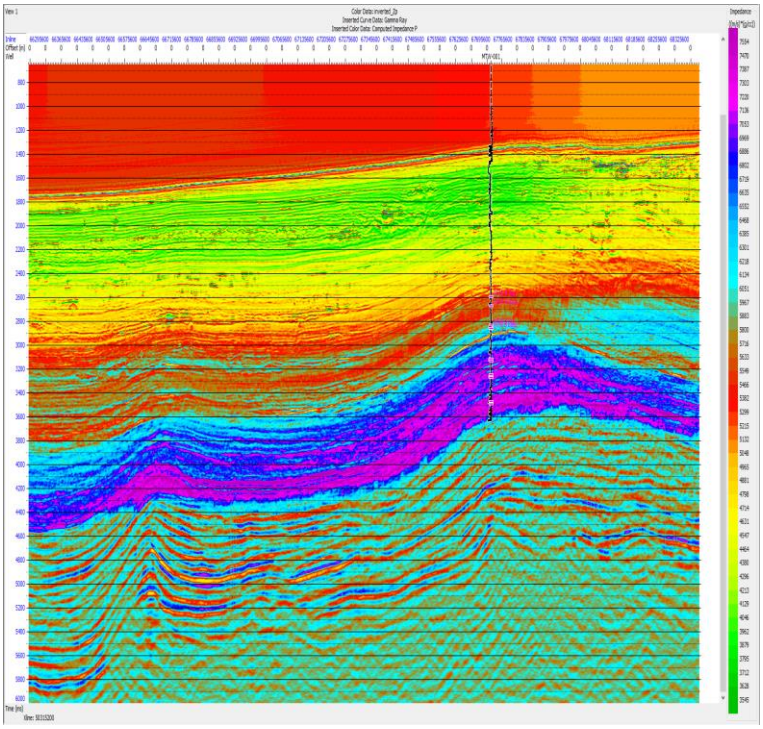

Fig. 14: 3-D Acoustic Impedance Cube with MTW-001 Well Inserted.

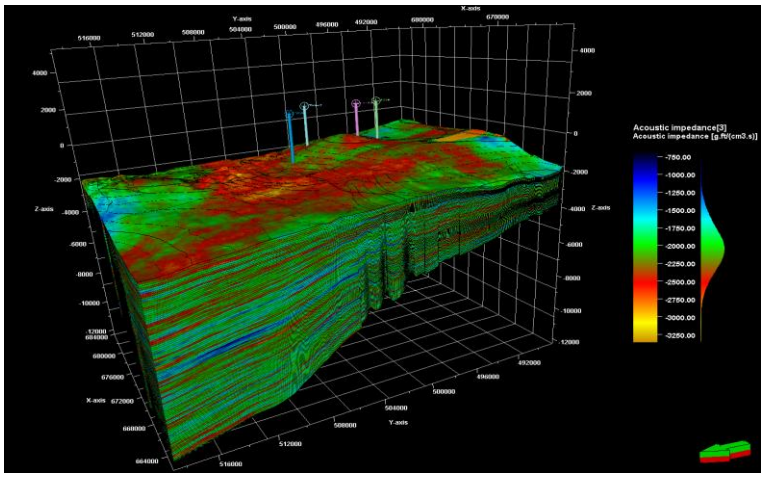

Fig. 15: 3-D Acoustic Impedance Cube Model Distributed Across Reservoir Nel_1902.

7. Conclusion

The study integrated the workflow above, to characterize the reservoir, from petrophysical analysis, seismic interpretation, surface attribute analysis, 3-D static model, and seismic inversion, through the integration of field data for accurate well placement.
The petrophysical research revealed that the five reservoir units defined had good reservoir quality, with high effective and total porosity, good permeability, and low water saturation. According to the findings of this study, the field average Net-to-gross, Effective porosity, Total porosity, Water saturation and Permeability are 90%, 27%, 32%, 44% and 2491.58 mD respectively. The form and structures of reservoir were established using fault structures in a 3-D static model built from the input of obtained data, while the limits of the structures assisted in the characterization of the formation top and base surfaces inferred from 3-D seismic data. The faulting model, 3-D pillar grid, horizon model, zoning, layering, property model and petrophysical model deliverables were all used to define the 3-D geological model built, the volumes of hydrocarbon estimated are STOIIP of 14.5 MMstb and reserve of 23.43 MMbo (RF- 40%) as resource evaluation of reservoirs in MTW Field. From impedance cube result, probable hydrocarbon accumulation was observed in the zones characterized by low P-impedance from green to red colour code. These zones are inferred to be hydrocarbon zones based on the low P-impedance values, while high P-impedance values depicted from cyan to purple code are indicative of shale- rich regions. The RMS amplitude result revealed high amplitude reflectivity which is a measure of zone of interest. Based on this, seven (7) prospects and three (3) leads were identified. The seismic inversion result shows a high level of accuracy with a correlation coefficient of 0.997; 0.997; 0.995; 0.996 in MTW-001, MTW-003ST1, MTW-004ST1 and MTW-005 wells, respectively. The acoustic impedance successfully resolved and improved on the resolution of the seismic stacking velocity especially at reservoir layers and at depth deeper than 3600 ms. Acoustic impedance being a layer property, has shown improvement on the lateral and vertical resolutions of the data beyond what the usual seismic interval velocity could image. This study has shown that uncertainty can be reduced by a blend of RMS amplitude and seismic inversion in identifying reservoirs for accurate placement of wells. Thus, this integrated approach should be adopted to de-risk any prospect and boost investors' confidence.

8. Declaration of interests

- The authors declare that they have no known competing financial interests or personal relationships that could have appeared to influence the work reported in this paper.
- The authors declare the following financial interests/personal relationships which may be considered as potential competing interests.

9. Conflict of interest

The author(s) declare(s) that there are no conflicts of interest regarding the publication of this article

References

[1] Archie, G. E. (1942). The Electrical Resistivity Log as an aid in determining some reservoir characteristics. *Journal of Petroleum Technology*, Vol.5: pp.54-62. https://doi.org/10.2118/942054-G.
[2] Beka F.T., and Oti, M.N. (1995). The Distal Offshore Niger Delta: Frontier Prospects of a Mature Petroleum Province, In: M. N. Oti and G. Postma, Eds., Geology of Deltas,. *A. A. Balkema, Rotterdam*. 237-241.
[3] Doust H., and Omatsola E. Niger Delta In: Edwards, J. D., and Santogrossi, P.A. (1990). eds., Divergent/passive Margin Basins . *AAPG*, Memoir. 48:.239-248. https://doi.org/10.1306/M48508C4.
[4] Ejedawe, J.E., Coker, S.J.L., Lambert-Aikhionbare, D.O, Alofe, K.B. and Adoh, F.O. (1984). Evolution of Oil Generating Window and Gas Evolution of Oil Generating Window and Gas. *AAPG Bulletin*. 68: 1744-1751.
[5] Ekweozor, C. M., and Daukoru, E. M. (1994). Northern delta Depobelt portion of the Akata – Agbada Petroleum system, Niger Delta: In Magoon, L.B. and Dow, W.G. (Eds). The petroleum system from source to trap. *American Association of Petroleum Geologists Memoir*. 1994. 460: 599 – 613. https://doi.org/10.1306/M60585C36.
[6] Evamy, B.D., Haremboure, J., Kamerling, P., Knaap, W.A., Molloy, F.A., and Rowlands, P.H. (1978). Hydrocarbon habitat of Tertiary Niger Delta. *American Association of Petroleum Geologists Bulletin*. 62: 277-298. https://doi.org/10.1306/C1EA47ED-16C9-11D7-8645000102C1865D.
[7] Farfour, M., Wang, Y. J., and Kim, J. (2015). Seismic attributes and acoustic impedance inversion in interpretation of complex hydrocarbon reservoirs. *Journal of Applied Geophysics*. 114:.68-80 https://doi.org/10.1016/j.jappgeo.2015.01.008.
[8] Hilchie, D. W. (1978). Applied Openhole Log Interpretation (for Geologists and Petroleum Engineers). *Geophysical well logging*. pp 1 - 350

[9] Hospers, J. (1965). Gravity Field and Structure of the Niger Delta, Nigeria, West Africa. *Geological Society of American Bulletin*. 76: 407-422. https://doi.org/10.1130/0016-7606(1965)76[407:GFASOT]2.0.CO;2.
[10] Kaplan A., Lusser C.U, and Norton I.O. (1994). Tectonic Map of the World, Panel 10. *American Association of Petroleum Geologists, Tulsa*. Scale 1:10,000,000.
[11] Klett T.R.,Thomas S. Ahlbrandt, J.W. Schmoker and Dolton, J.L. (1997). Ranking of the world's oil and gas provinces by known petroleum volumes. *U.S. Geological Survey Open-file Report-97-463, CD-ROM*. 56 – 58. https://doi.org/10.3133/ofr97463.
[12] Kulke, H. (1995). Nigeria. In: Kulke, H., Ed., Regional Petroleum Geology of the World, Part II: Africa, America, Australia and Antarctica. *Berlin, Gebruder Borntraeger*. 143-172.
[13] Maurya, S. P., and Sarkar, P. (2016). Comparison of Post stack Seismic Inversion methods: A case study from Blackfoot Field, Canada. *Journal of Scientific & Engineering Research*, 7:1091-1101.
[14] Nwachukwu, J. I. and Chukwurah, P. I. (1986). Organic Matter of Agbada Formation, Niger Delta, Nigeria. *AAPG Bulletin*. 70: 48-55 https://doi.org/10.1306/94885624-1704-11D7-8645000102C1865D.
[15] Olowoyo K. O. (2010). Structural and Seismic Facies Interpretation of Fabi Field, Onshore, Nigeria Delta. *Boca Raton, Florida, USA*. 1-25.
[16] Othman, A. A. A., Ewida, H. F., Fathi Ali M. M., and Embaby M. M. A. A. (2017). Reservoir Characterization Applying Seismic Inversion Technique and Seismic Attributes for Komombo Basin. *Austin Journal Earth Science*, 3(1):1020.
[17] Petroconsultants. (1996). Petroleum exploration and production database: Houston, Texas. *Petroconsultants, Inc*, P.O. Box 740619, Houston, TX 77274-0619.
[18] Short, K, and Stauble, A. (1967). Outline of geology of Niger Delta. *American Association of Petroleum Geologists Bulletin.* 51:761–779. https://doi.org/10.1306/5D25C0CF-16C1-11D7-8645000102C1865D.
[19] Stacher, P. (1995). Present understanding of the Niger Delta hydrocarbon habitat, In, M. N Oti and G. Postma (eds.), Geology of Deltas. *Rotterdam, AA Balkema*. 257–267.
[20] Veeken, P. C. H. and Da Silva, M. (2004). Seismic inversion methods and some of their constraints: Fisrt Break. *https://www.researchgate.net/publication/277392423*, 22:47-70. https://doi.org/10.3997/1365-2397.2004011.